

Spectral Analysis of Noise LC-Oscillators – New Thoughts on an Old Subject

Aleksandar Tasić, Wouter A. Serdijn and John R. Long

Abstract — Resonant-inductive degeneration of bias current source is described in this paper as a method for a manifold improvement of phase noise in LC voltage-controlled oscillators. The design procedure is based on a phase-noise model obtained from the spectral analysis of noise in oscillators. By forming a resonance at twice the oscillation frequency in the emitter of the bias current source transistor, phase noise of degenerated oscillator is improved by 6dB, resulting in -112dBc/Hz at 1MHz offset from a 5.7GHz-band carrier, while drawing 4.8mA from a 2.2V supply. The test oscillator achieves a frequency tuning range of 600MHz, between 5.45-6.05GHz.

Index Terms — voltage-controlled oscillator, noise factor, phase noise, resonant-inductive degeneration.

I. INTRODUCTION

IN a high-performance oscillator circuit [1], the contribution of the bias current source noise of an LC voltage-controlled oscillator (VCO) to the phase noise is larger than all other noise contributions put together (i.e., LC-tank noise and transconductor noise). Therefore, the noise-optimization procedure proposed in this paper is focused on reducing noise generated by the bias current source. Resonating a degeneration inductor in emitter of the bias transistor with its base-emitter capacitance at twice the oscillation frequency ($2f_0$) effectively reduces its output noise that would otherwise be converted by hard switching of the oscillator transconductor into phase noise. We call this “resonant-inductive degeneration” (RID) [1]. It is suitable for low-voltage applications, as it requires no D.C. voltage headroom. It allows for a manifold improvement of oscillators’ phase-noise.

The design procedure of the oscillator with resonant-inductive degeneration is based on the phase-noise model and spectral noise analysis [2]. This phase-noise model is amenable for design as it describes the noise performance of LC-VCOs qualitatively and quantitatively using electrical parameters.

Contributions of all noise sources to the phase noise of bipolar LC-oscillators are briefly reviewed in Section II. Section III details on the application of the phase-noise model obtained to improve phase noise in bipolar LC-oscillators by

means of resonant-inductive degeneration. Oscillator circuit parameters and experimental results are presented in Section IV.

II. PHASE-NOISE MODEL

A bipolar LC voltage-controlled oscillator, shown in Fig. 1, is used for phase-noise analysis. It consists of a resonant LC tank, a capacitive voltage divider (C_A , C_B), and a cross-coupled transconductance amplifier (Q_1 , Q_2). The bias current source provides current I_{TAIL} . L is the tank inductance, C the tank capacitance, R_{TK} the effective tank resistance, n the capacitive divider ratio, g_m the transconductance of bipolar transistors Q_1 , Q_2 , and k the small signal loop gain.

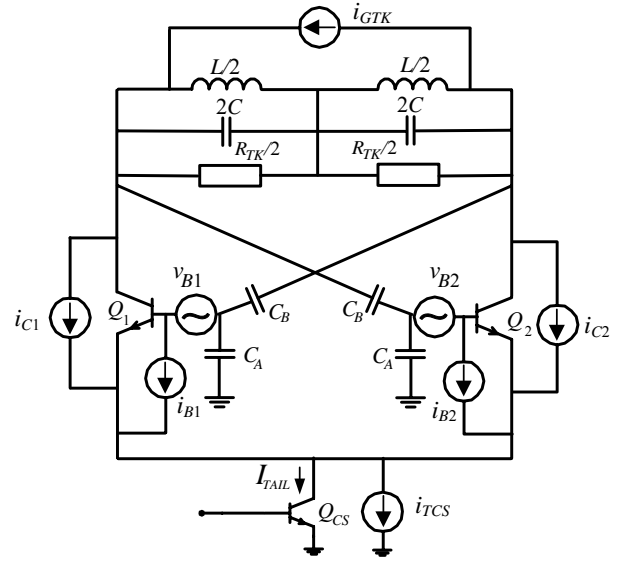


Fig. 1: Bipolar LC-VCO and its main noise sources.

The noise sources shown are the tank-conductance current noise source (i_{GTK}), the base-resistance (r_B) thermal noise source (v_B), the collector-current (i_C), and the base-current (i_B) shot noise sources, and the equivalent output current noise (i_{BCS}) of the bias current source transistor Q_{CS} .

Single-sided phase noise (\mathcal{L}) at the output of the resonator at a frequency $f_0 + \Delta$ is defined as

$$\mathcal{L} = \frac{|Z(f_0 + \Delta)|^2 i_{PM,TOT}^2}{v_s^2 / 2}. \quad (1)$$

A. Tasić, W. A. Serdijn and J. R. Long are with Delft University of Technology, Department of Microelectronics, Mekelweg 4, 2628CD Delft, The Netherlands, Boulder, CO 80305 USA (phone: +31152781579; fax: +31152785722; e-mail: a.tasic@tudelft.nl).

$Z(f_0+\Delta)$ is the equivalent tank impedance at an offset frequency Δ from the resonant frequency f_0 , $i_{PM,TOT}^2$ is the single-sided phase-related noise power at the output of the transconductance cell, and v_S is the amplitude of the voltage swing across the resonator.

We will first derive a duty cycle of a time-varying small-signal g_m -cell gain, its Fourier series, and a Fourier series of a large-signal g_m -cell switching characteristic for bipolar case. Then, we will determine the contributions of the oscillator noise sources to the phase noise at the LC-tank ($i_{PM,TOT}$) and finally the phase-noise model.

A. Time-Varying Small-Signal g_m -Cell Gain

The nonlinear voltage-to-current transfer function (referred to the LC-tank) of the transconductor, its equivalent time-varying small-signal transconductance in the presence of a large driving signal, and (large-signal) current through the resonator are shown in Figs. 2a, 2b, and 2c, respectively.

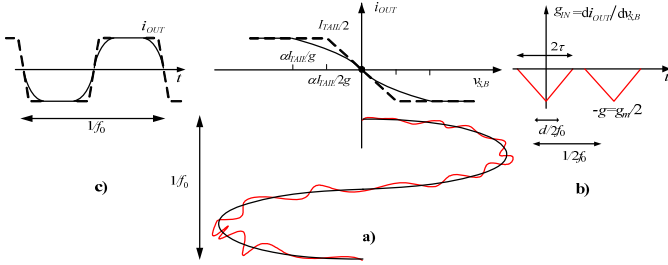


Fig. 2: a) Large-signal V -to- I characteristic with b) small-signal time-varying gain of the g_m -cell in the presence of a large oscillation signal, and c) current through the resonator.

As long as the oscillation signal across the bases of the g_m -cell ($v_{S,B}$) is not clipped, the transconductor gain for the accompanying noise signal has a linearly decaying gain value. When limiting occurs, the small-signal gain reduces to zero. If period of the oscillation signal is $1/f_0$, the period of the small-signal time-varying gain (g_{IN}) is $1/(2f_0)$. Considering the transformation from the bases to the collectors of the transconductor Q_1 - Q_2 , the small-signal gain g is $g_m/2$.

Let us now determine the average value and normalized power of the time-varying gain function shown in Fig. 2b, which will be used in the noise analysis.

If d is a duty cycle and 2τ a width of the triangular-wave function $g_{IN}(t)$, its average value $g_{\nabla,0}$ is given by Eqs. (2).

$$g_{\nabla,0} = \frac{1}{T_2} \int_{-T_2/2}^{T_2/2} g_{\nabla}(t) dt = \frac{2}{T_2} \int_0^{\tau} g \left(1 - \frac{t}{\tau}\right) dt = gd \quad (2)$$

If $\pm 2\alpha V_T$ is the linear region of the transconductor large-signal characteristic (dashed V -to- I function of Fig. 2a), the

effective duty cycle of the triangular-wave time-varying gain can be expressed as

$$d = \frac{2\tau}{T_0} = \frac{2}{\pi} \arcsin \left(\frac{2\alpha V_T}{v_{S,B}} \right). \quad (3)$$

The voltage swing across the LC-tank is defined as the product of the tank resistance $1/G_{TK}$ and the first Fourier coefficient of the current I_1 through the tank,

$$v_S = I_1 R_{TK}. \quad (4)$$

For a large value of the oscillator small-signal loop gain k , output current i_{OUT} is described by a close-to-square wave with amplitude $I_{TAIL}/2$ (see Fig. 2c). Component I_1 now equals the first harmonic of the current signal shown. With the aid of Eqs. (2-4), the voltage swing across the resonator v_S then reads

$$v_S = \frac{2}{\pi} I_{TAIL} R_{TK} = \frac{8}{\pi} knV_T = nv_{S,B}. \quad (5)$$

Assuming a 100mV ($\pm 2V_T$) bipolar transconductor linear region (dashed line of Fig. 2a, [17]) and a large loop-gain value, the duty cycle d can be approximated as

$$d = \frac{1}{2k}. \quad (6)$$

This expression describes the relationship between the small-signal loop gain and duty cycle for $k \gg 1$, hard switching of the g_m -cell, and large oscillation signal generated.

The average normalized power of the time-varying gain function, P_{∇} , is given by Eqs. (7).

$$P_{\nabla} = \frac{1}{T_2} \int_{-T_2/2}^{T_2/2} g_{\nabla}^2(t) dt = \frac{2}{T_2} \int_0^{\tau} g^2 \left(1 - \frac{t}{\tau}\right)^2 dt = \frac{2}{3} g^2 d \quad (7)$$

In the remainder of this section, we will first determine Fourier coefficients of the triangular small-signal g_m -cell gain. Then, harmonic components of the large-signal g_m -cell transfer function are calculated. Harmonics of the corresponding gain functions are needed for the spectral noise analysis and derivation of phase noise [2].

B. Fourier Coefficients of the Time-Varying Small-Signal g_m -Cell Gain

The noise from the LC-tank and transistors Q_1 and Q_2 is modulated by the frequency of the time-varying gain g_{IN} . Consequently, *noise folding* occurs, i.e., g_m -cell noise from a number of frequencies is converted into the phase-noise at one

frequency. In order to calculate noise contributions of the g_m -cell and LC-tank to the resonator phase-modulating component, a frequency domain small-signal transfer function of the g_m -cell shown in Fig. 2b has to be determined.

Magnitudes of the harmonic components of the complex Fourier development for the time-varying gain g_{IN} are shown in Fig. 3 and given by Eq. (8).

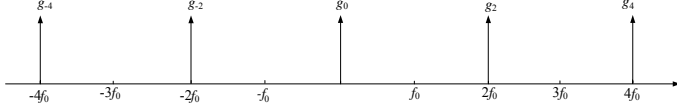


Figure 3: Magnitudes of complex Fourier series of the g_m -cell small-signal gain for $k \gg 1$.

$$g_{2i} = gd \left(\frac{\sin(i\pi d)}{i\pi d} \right)^2 \quad (8)$$

Gain g_{IN} has harmonic components at even multiples of the oscillation frequency only (multiples of $2f_0$). For the sake of simplicity, all coefficients are used positive (as magnitudes) in the spectral representations.

For $k \gg 1$, Eq. (8) simplifies to

$$g_{2i} = gd = \frac{g_m}{2} d, \quad (9)$$

for the components upto the vicinity of a zero crossing of the envelope *sinc* function of Eq. (8) that is reached at a frequency $2f_0/d$ (see Fig. 2).

C. Fourier Coefficients of the Large-Signal g_m -Cell Gain

The noise of the bias current source is switched on/off (± 1 wave) by the f_0 -periodic transconductor limiting characteristic, shown in Fig. 2c. This results in the folding of the bias current source noise.

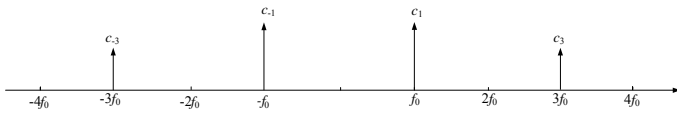


Fig. 4: Magnitudes of the complex Fourier series of the transconductor large-signal switching characteristic.

The complex Fourier coefficients of the square-wave switch function (see Fig. 2c) are positioned at odd multiples of the oscillation frequency as depicted by Fig. 4. Their magnitudes (thus positive real numbers) are defined by Eq. (10) for $k \gg 1$.

$$c_{2i+1} = \left| \frac{\sin((2i+1)\pi/2)}{(2i+1)\pi/2} \right| \quad (10)$$

D. Oscillator Noise Factor and Phase Noise

Noise factors of the LC-tank loss conductance, g_m -cell collector current shot noise and base resistance thermal noise, and bias current source noise are formulated in this section. The phase-noise model, accounting for all noise contributions, is then calculated.

The contribution of the LC-tank noise to the phase noise, prior to shaping by the LC-tank impedance $Z(\Delta\omega)$, equals [2]

$$\mathcal{L}(R_{TK}) = \frac{4KTG_{TK}}{v_s^2}. \quad (11)$$

If we relate the contribution of each noise source n to the phase noise by a noise factor $F(n) = v_s^2 \mathcal{L}(n) / (4KTG_{TK})$, from Eq. (11), we obtain the LC-tank noise factor $F(R_{TK})$ as

$$F(R_{TK}) = \frac{v_s^2 \mathcal{L}(R_{TK})}{4KTG_{TK}} = 1. \quad (12)$$

The base-resistance thermal noise components at odd multiples of resonant frequency fold to the resonator via the even-order harmonic components of the small-signal time-varying gain of the g_m -cell (see Fig. 3) [2].

Taking into account both transistors of the g_m -cell, the total base-resistance phase-noise contribution is given by a noise factor $F(2r_B)$, derived with the aid of Eq. (7),

$$F(2r_B) = \frac{v_s^2 \mathcal{L}(2r_B)}{4KTG_{TK}} = \frac{2}{3} nkc, \quad (13)$$

where $c = r_B 2nG_{TK}$ is a start-up constant.

This result suggests that the contribution of the base-resistance noise to the phase noise of the oscillator under consideration is directly proportional to the loop gain k (thus power consumption) and the parameters n and c , the latter relating the base resistance of the transconductor transistors and the quality of the resonator.

Taking into account contributions of collector-current shot-noise sources from both transconductor transistors, a noise factor $F(2I_C)$ is obtained from Eq. (14) [2], using Eq. (2).

$$F(2I_C) = \frac{v_s^2 \mathcal{L}(2I_C)}{4KTG_{TK}} = \frac{n}{2} \quad (14)$$

This suggests that the phase-noise contribution of the g_m -cell collector-current shot-noise is independent of loop gain and power consumption, but a capacitive divider ratio n .

Folding of the bias current source noise is a result of operation of the g_m -cell in the limiting region. The transconductor switching function (see Fig. 4) converts the bias current source noise around odd multiples of the

oscillation frequency back to the LC-tank at the oscillation frequency f_0 [2].

The resulting noise factor $F(I_{BCS})$ is given bellow.

$$F(I_{TCS}) = k\left(\frac{n}{2} + nkc\right) \quad (15)$$

Without loss of generality, we use $g_{m,CS}=2g_m$ and assume $2r_{B,CS}=r_B$, given the same transit frequencies (f_T) of transistors Q_1 , Q_2 and Q_{CS} .

Assumed to be uncorrelated, all noise sources, viz., the tank conductance noise, the base resistance noise, the transconductor shot noise, and the bias current-source noise add up to an equivalent phase-modulating component. With the aid of Eqs. (12)-(15), the noise factor of the bipolar LC oscillator now becomes as given by Eqs. (16) and (17).

$$F = F(R_{TK}) + F(2I_C) + F(2r_B) + F(I_{BCS}) \quad (16)$$

$$F = 1 + (1+k)\frac{n}{2} + \left(\frac{2}{3} + k\right)nkc \quad (17)$$

The phase noise is determined with the aid of Eq. (1) as

$$\mathcal{L} = \frac{4KTG_{TK}}{(4\pi C_{TOT}\Delta)^2} \left(\frac{\pi}{8V_T}\right)^2 \frac{1 + (1+k)\frac{n}{2} + \left(\frac{2}{3} + k\right)nkc}{k^2 n^2}. \quad (18)$$

The result obtained is an intuitive description of the phase-noise phenomenon in the LC oscillator under consideration. The model developed doesn't require use of numerical solvers, yet providing oscillator designers with a valuable tool for analysis and synthesis of high-performance oscillators.

It is important to note that Eqs. (18) is the worst-case noise factor of the bipolar oscillator under consideration, thereby overestimating its phase noise performance. The loop-gain related contributions, viz., the base-resistance noise contribution of the transconductor, Eq. (13), and the base-resistance and collector-current noise contributions of the bias current source, Eq. (15), are calculated implicitly assuming infinite bandwidth of both the noise sources and the operation of the oscillator devices.

E. Oscillator Phase-Noise Model - Discussion

To describe the relationship between the corresponding phase-noise contributions, we introduce the phase-noise ratio, PNR . It is a ratio of phase noise of oscillators with bias current-source noise present (current source shown in Fig. 1) and removed (ideal, noiseless current source), respectively, as given by Eq. (19),

$$PNR = 1 + \frac{k\left(\frac{n}{2} + nkc\right)}{1 + \frac{n}{2} + \frac{2}{3}nkc} \cong 1 + k \frac{F(2I_C, 2r_B)}{1 + F(2I_C, 2r_B)}, \quad (19)$$

where $F(2I_C, 2r_B)$ is the noise factor of the g_m -cell. It is now easy to conclude that failing to suppress the noise contribution of the BCS to the phase noise, a factor in the order of k degraded performance results. Thus, for a typical loop gain of around 10, a consequence of the BCS noise present is a degradation of the phase noise of ~ 10 dB, as suggested by Eq. (19), even for a high-quality LC-tank designed.

To confirm these findings, the oscillator shown in Fig. 1 is simulated using SpectreRF with the following parameters: oscillation frequency $f_0 \sim 5.74$ GHz, tank resistance $R_{TK} \sim 340\Omega$, capacitive divider ratio $n \sim 1.65$, start-up constant $c \sim 0.25$, supply voltage $V_{CC} = 2.2$ V.

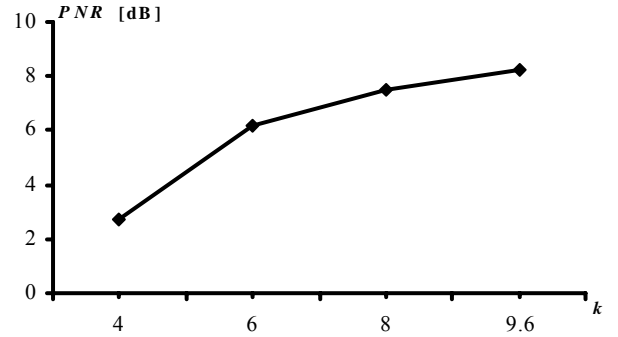


Fig. 5: Simulated phase-noise ratio.

At the maximum loop gain of around 10, the noise from the BCS degrades the phase noise of the oscillator under consideration for 8.2dB in the simulations (8.7dB calculated), as shown in Fig. 5. At the maximum loop gain considered, the BCS noise accounts for around 85%, the g_m -cell noise for around 10%, and the LC-tank noise for 5% of the phase-related noise power.

III. RESONANT-INDUCTIVE DEGENERATION

We will determine the performance of resonant-inductive degeneration by calculating transfer functions from the base-resistance noise, base-current shot noise, and collector-current shot noise sources to the output of the current source using a detailed schematic shown in Fig. 6.

Using superposition, total output noise of the bias current source with resonant-inductive degeneration will be then determined, and formulations for the oscillator noise factor and phase noise adapted.

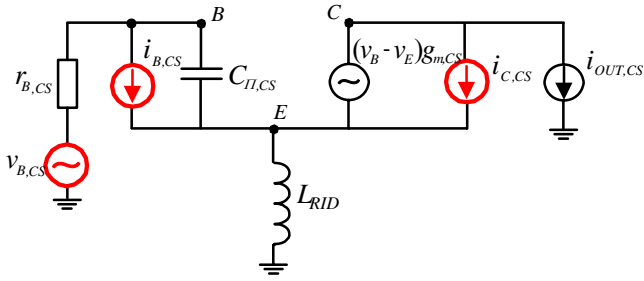


Fig. 6: Circuit of the bias current source with RID.

A. Transformation of the BCS Base-Resistance Noise

The contribution of the noise from the base resistance to the output current noise density $i_{OUT,CS}$ of the degenerated bias current source can be calculated from Fig. 6 as [1]

$$\frac{i_{OUT,CS}}{v_N(r_{B,CS})}(2f_0) = -g_{m,CS} \frac{2f_0}{f_{T,CS}}. \quad (20)$$

This suggests that a reduction of the bias current source base-resistance thermal noise is possible for $2f_0/f_{T,CS} < 1$.

B. Transformations of the BCS Base- and Collector-Current Shot Noise Sources

The RID bias current source transistor Q_{CS} operates in a common-base-like configuration at the resonance at twice the oscillation frequency. Referred to the output of transistor Q_{CS} , we expect to see the collector-current shot noise suppressed and the base-current shot noise present. This intuitive observation can be analytically proved with the aid of Fig. 6. We will first determine the transfer function for collector-current shot noise $i_{C,CS}$ to the output of the current source $i_{OUT,CS}$ by applying superposition (i.e., $i_{B,CS}=0$ and $v_{B,CS}=0$).

The transfer function from the collector-current noise source to the output of the BCS is at the resonance ($2f_0$) between L_{RID} and $C_{\pi,CS}$ calculated as

$$\frac{i_{OUT,CS}}{i_N(I_{C,CS})}(2f_0) = 1 - \frac{1}{1 + r_{B,CS}g_{m,CS}\left(\frac{2f_0}{f_{T,CS}}\right)^2} \cong 0. \quad (21)$$

As $r_{B,CS}g_{m,CS}$ is a small constant (equals ck for $2r_{B,CS}=r_B$) and $2f_0/f_{T,CS} \ll 1$, the collector-current shot noise can be suppressed from the output of the BCS.

In a similar manner, the transformation of the base-current shot noise to the output of the BCS is calculated from Fig. 6 ($i_{C,CS}=0$ and $v_{B,CS}=0$). The resulting transfer function at resonance ($2f_0$) reads

$$\frac{i_{OUT,CS}}{i_{B,CS}}(2f_0) = \frac{1}{1 + r_{B,CS}g_{m,CS}\left(\frac{2f_0}{f_{T,CS}}\right)^2} \cong 1. \quad (22)$$

This implies that the base-current shot noise is transferred completely to the output of the degenerated bias current source.

C. Noise Factor of the RID BCS

Combining the base-resistance noise and the base-current shot noise contributions, Eqs. (20) and (22), the total output current noise density of the resonant-inductive degenerated bias current source becomes

$$i_N^2(I_{TCS,RID}) = 2kT \frac{g_{m,CS}}{2} \left[0 + \left(\frac{f_{T,CS}}{2f_0}\right)^2 \frac{1}{\beta} + 2r_{B,CS}g_{m,CS} \right] \left(\frac{2f_0}{f_{T,CS}}\right)^2 \quad (23)$$

The noise factor of the bias current source with resonant-inductive degeneration now equals

$$F(I_{BCS,RID}) = k \cdot \left[\frac{n}{2\beta} \left(\frac{2f_{T,CS}}{f_0}\right)^2 + nk \right] \left(\frac{2f_0}{f_{T,CS}}\right)^2. \quad (24)$$

Resonant-inductive degeneration suppresses most effectively bias current noise around second harmonic of the oscillation frequency by forming a resonance, but also the BCS noise from higher harmonics ($4f_0, 6f_0, \dots$). The BCS noise around $2f_0$ is responsible for around 72% [2] of the total bias noise, which is reduced by a factor $(f_{T,CS}/2f_0)^2$ after the RID. The smaller portion of the BCS noise ($\sim 28\%$) originates from higher harmonics, which is reduced by forming a high impedance in emitter of the BCS transistor ($\sim 4\omega_0 L_{RID}$ at $4f_0, 6\omega_0 L_{RID}$ at $6f_0, \dots$), that is, the gain for thermal base-resistance noise to the output of the BCS is small and the flow of collector-current shot noise impeded.

In order to estimate the improvement achieved, Eq. (24) is compared to the output current noise density of the BCS without degeneration, given by Eq. (25).

$$i_N^2(I_{BCS}) = 2kT \frac{g_{m,CS}}{2} \left[1 + 0 \cdot \left(\frac{f_{T,CS}}{2f_0}\right)^2 \frac{1}{\beta} + 2r_{B,CS}g_{m,CS} \right] \quad (25)$$

A comparison between Eqs. (24) and (25) suggests that by applying resonant-inductive degeneration, the contribution of the bias current source noise is reduced more than a factor $(f_{T,CS}/2f_0)^2$.

For example, a factor 25 reduction of the BCS noise is possible for $f_{T,CS}=10f_0$. Minimizing or eliminating the noise contribution of the BCS improves phase noise performance of the oscillator, or it permits operation at a lower bias current

for the same performance of the oscillator under consideration.

The phase-noise ratio between oscillators with an RID BCS, Eq. (26), and an ideal (i.e., noiseless) bias current source now equals

$$PNR = 1 + \frac{k\left(\frac{n}{2} + nkc\right)\left(\frac{2f_0}{f_{T,CS}}\right)^2}{1 + \frac{n}{2} + \frac{2}{3}nkc}. \quad (26)$$

For $2f_0/f_{T,CS} \ll 1$, which is readily achievable, the BCS noise contribution can be eliminated, whereby the noise factor and phase noise of the oscillator with RID BCS become

$$F \cong 1 + \frac{n}{2} + \frac{2}{3}nkc, \quad (27)$$

and the phase-noise ratio reduces to $PNR \sim 1$. In this case, the phase noise of the LC oscillator of Fig. 1 with a bias current source of Fig. 6 is

$$\mathcal{L} = \frac{4KTG_{TK}}{(4\pi C_{TOT}\Delta)^2} \left(\frac{\pi}{8V_T}\right)^2 \frac{1 + \frac{n}{2} + \frac{2}{3}nkc}{n^2k^2}. \quad (28)$$

For a high-performance LC-tank designed ($c \ll 1$), the phase noise of a bipolar LC oscillator with a common-emitter bias transistor is proportional to $1/k$, given $k \gg 1$ (see Eq. (18)). However, biasing the same oscillator circuit with an inductor-degenerated transistor, the phase noise becomes proportional to $1/k^2$ (see Eq. (28)), a factor of k improvement.

IV. DESIGN OF LC-OSCILLATORS WITH RID BCS

A. Oscillator Circuit Parameters

For a supply voltage of 2.2V, a transistor base bias voltage V_B of around 1.85V is chosen. It allows for both the largest voltage swing of the output signal and the most efficient use of the voltage headroom available. Maximum voltage swing is estimated from the saturation condition of the transistor transistors, in order to avoid noise injection of the forward-biased base-collector junctions. For a tapped capacitor ratio $n = 1 + (C_A + C_D)/C_B$ of 1.6, a maximum voltage swing across the bases of the transistor $v_{S,B,MAX}$ of around 0.68V is expected, corresponding to a small-signal loop gain of around 10.

For effective suppression of the bias current source noise at twice the oscillation frequency (i.e., between 11GHz and 12GHz), a symmetric resonant-degenerative inductor of 2.6nH ($2 \times L_{RID}$) was integrated in a 1.25μm thick metal. It has 7 turns, outer diameter of 106μm, metal width of 5μm, and metal spacing of 1.5μm. A small resistor (30Ω) was added in series with the degenerative inductor. Although this has minor effect

on high-frequency bias current noise, it aids suppression of low-frequency BCS noise and improves temperature stability of the oscillator.

As a compromise between low phase noise, low power consumption and frequency tuning range (aiming for the upper 802.11a/HIPERLAN/802.16a [3,4,5] band), the other oscillator parameters have been determined. The 1.2nH LC-tank inductor was designed using 4μm thick aluminum top metal in the 120GHz SiGe technology [6]. This differentially shielded symmetric 2-turn inductor uses a ladder substrate shield, has an outer dimension of 190μm, metal width of 10μm, and metal spacing of 5μm. Two n-type MOS varactors with 40 gates are used to tune the LC-tank. Metal-insulator-metal capacitors C_A and C_B are 100fF and 250fF, respectively.

Two common-collector output buffers interface the oscillator and a 50Ω measurement set-up, each consuming 1.1mA of current.

B. Experimental Results

The chip photomicrograph of the voltage-controlled oscillator with resonant-inductive degeneration is shown in Fig. 7 (together with buffer circuits) [1].

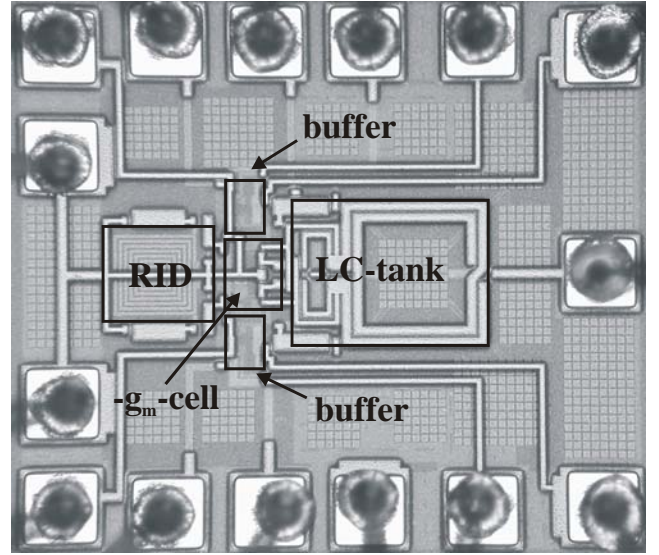


Fig. 7: Photomicrograph of the LC-VCO with RID.

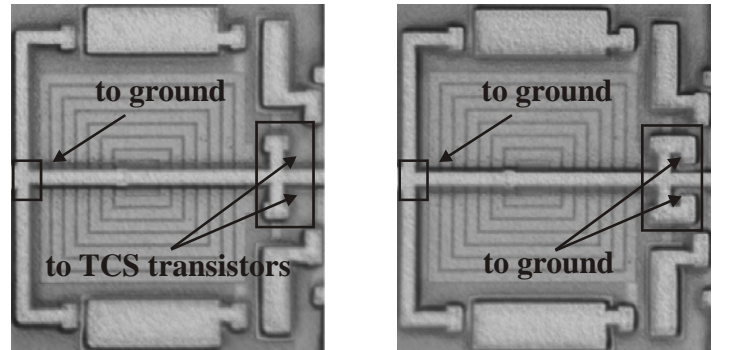


Fig. 8: (left) VCO with RID, (right) VCO without RID.

Oscillator and buffers occupy an area of $215 \times 490 \mu\text{m}^2$ (0.1mm^2), excluding bondpads. For validation of the resonant-inductive degeneration method, another (identical) voltage-controlled oscillator was designed without resonant-inductive degeneration (i.e., L_{RID} is grounded on both sides), as shown in Fig. 8. The two oscillator designs have maximum voltage swing and lowest phase noise for the same power consumption, as they have identical LC-tanks, transconductors, and bias current source transistors.

After wirebonding into 32-lead quad packages, the oscillator designs were connected to a printed-circuit board with bias and supply line filtering for testing.

A frequency tuning range of 600MHz (5.45GHz-6.05GHz) was measured for a 0.9V tuning voltage range (i.e., between 1.3V and 2.2V) as seen in Fig. 9. The error on the prediction of the oscillation frequency is below 1%. This frequency tuning range covers the upper band of 802.11a/HIPERLAN/802.16a, and with additional MOS capacitors in parallel with the LC-tank the operating frequency could be trimmed to cover the complete 5GHz band. Combined with an injection-lock oscillator [7], this design allows for a multistandard operation (i.e., 802.11a/HIPERLAN/802.16a and HIPERLINK modes) as it would be able to cover the 17.1-17.3GHz band with a large margin.

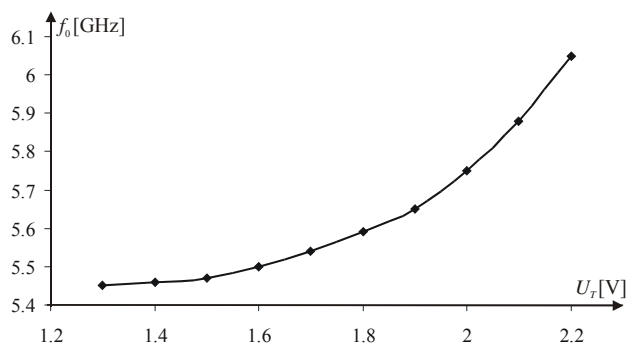


Fig. 9: VCO frequency tuning characteristic.

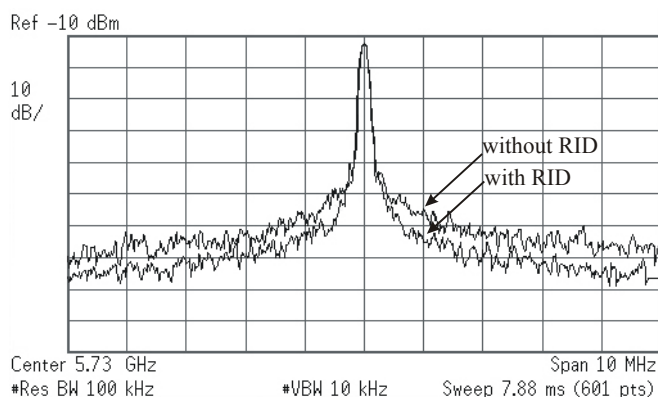


Fig. 10: Oscillators' outputs in a 5.7GHz band.

Phase noise properties of the oscillators with and without RID are compared in Fig. 10. The oscillator with the resonant-inductive degenerated bias current source has around 6dB

better phase noise at 1MHz offset from the carrier in the 5.7GHz band, compared to the oscillator implemented without RID.

At 1MHz offset in the upper 5.7GHz band, the oscillator with the resonant-inductive degenerated bias current source achieves a phase noise of -112dBc/Hz for a current consumption of 4.8mA.

V. CONCLUSIONS

It has been shown that the contribution of the bias current source noise to the phase noise of the LC-VCOs is larger than other noise contributions put together. We have proposed a method to reduce the phase-noise contribution of the bias current source by forming a resonance in its emitter at twice the oscillation frequency.

Resonant-inductive degeneration is suitable for low-voltage RF applications, as it requires no D.C. voltage headroom, and a low-nH inductor that can be cost-effectively implemented in any modern multi-layer metal silicon technology.

A 5.7GHz-band oscillator has been designed with a resonant-inductive degenerated bias current source to improve the phase noise of by 6dB, resulting in -112dBc/Hz phase noise at 1MHz offset for a power consumption of 10.6mW.

The design procedure is based on the phase-noise model derived for bipolar LC voltage-controlled oscillators.

REFERENCES

- [1] A. Tasić, W. A. Serdijn, J. R. Long and D. Haramé, "Resonant-Inductive Degeneration for a Fourfold Phase-Noise Improvement of a 5.7GHz Band Voltage-Controlled Oscillators", *Proceedings IEEE Bipolar/CMOS Circuit and Technology Meeting*, pp. 236-239, October 2005.
- [2] A. Tasic, W. A. Serdijn and J. R. Long, "Phase-Noise in LC-Oscillators - New Thoughts on an Old Subject", in submission to *IEEE Journal of Solid-State Circuits*, 2006/2007.
- [3] The IEEE 802.16 Working Group on Broadband Wireless Access Standards, <http://www.ieee802.org/16/>.
- [4] ETSI HIPERLAN/2 Standard, <http://portal.etsi.org/bran/kta/Hiperlan/hiperlan2.asp>.
- [5] *Wireless LAN MAC and Physical Layer (PHY) Specification – High-Speed PHY in the 5GHz Band*, ANS/IEEE Standard 802.11a, 1999.
- [6] A. Joseph et al., "A 0.18 μm 120/100GHz (f_T/f_{MAX}) HBT and ASIC-Compatible CMOS using Copper Interconnect", *Proceedings BCTM*, pp. 143-146, October 2001.
- [7] A. Tasic, S. Y. Yue, Sennis K. L. Ma, W. A. Serdijn, J. R. Long, and D. L. Haramé, "Receiver RF Front-End with 5GHz-Band LC Voltage-Controlled Oscillator and Subharmonically-Locked Ring Oscillator for 17GHz Wireless Applications", *Proceedings RFIC*, pp. 463-466, June 2006.